

Linkage between seasonal insolation gradient in the tropical northern hemisphere and the sea surface salinity of the equatorial Indian Ocean during the last glacial period

R. Saraswat^{1*}, R. Nigam¹, A. Mackensen², S. Weldeab³

¹ Micropaleontology Laboratory, National Institute of Oceanography, Goa, India

² Alfred Wegner Institute for Polar and Marine Research, Bremerhaven, Germany

³ Department of Earth Science, University of California, Santa Barbara, USA

(* For Correspondence: E-mail: rsaraswat@nio.org; rs.niog@gmail.com)

Abstract

Paired stable oxygen isotope and Mg/Ca analyses in calcite tests of mixed-layer dwelling planktic foraminifer *Globigerinoides ruber*, has been used to reconstruct equatorial Indian Ocean $\delta^{18}\text{O}$ of seawater ($\delta^{18}\text{O}_{\text{sw}}$) over the last ~137 kyr. On the basis of ice volume corrected $\delta^{18}\text{O}_{\text{sw}}$ ($\delta^{18}\text{O}_{\text{sw-ivc}}$), relative changes in sea surface salinity (SSS) have been estimated. The SSS estimates suggest three episodes of higher SSS (131-113 kyr BP, 62-58 kyr BP, and 30-24 kyr BP) within the last glacial period as compared to the present. The SSS comparison between the interglacial episodes reveals that the surface seawater over the core site was significantly saltier during penultimate interglacial than the Holocene. We suggest that the evolution of seasonal insolation gradient between the Indian monsoon areas and the equator over the investigated time interval was instrumental in shaping the strength of Indian winter and summer monsoons that left their imprints on the equatorial Indian Ocean SSS via fresh water input and wind-induced mixing. The study shows that the insolation difference between northern latitudes and equator during winter time affects the monsoon strength in the Indian region, especially during cold intervals.

Key words: Oxygen Isotope, Mg/Ca, *Globigerinoides ruber*, Salinity, Indian Ocean, Insolation

Introduction

The monsoon in Indian subcontinent comprise of two distinct phases, viz. summer monsoon, which at present brings >80% of the total precipitation, and winter monsoon that brings rainfall mainly along the southeastern coastal Indian region during winter season. The initiation and establishment of current monsoon regime with distinct summer and winter monsoon seasons in the Indian subcontinent has been proposed to be a consequence of the collision of the Indian plate with the Eurasian plate and subsequent uplift of the Tibetan plateau and northern hemisphere glaciation (Molnar et al. 1993; Prell and Kutzbach 1997; Gupta and Thomas 2003; Gupta et al. 2004). The relative strengths of summer and winter monsoon have varied during the past. On orbital time scales, there is a general consensus that the strength of Indian summer monsoon is linked to seasonal insolation changes over the region, with a strong (weak) summer (winter) monsoon during the interglacial (glacial) (Naidu and Malmgren 1996; Anderson et al. 2002; Gupta and Thomas 2003). In contrast, the winter monsoon is believed to intensify during cold interval (Duplessy 1982; Tiwari et al. 2005). However, the mechanism that controls winter monsoon precipitation is poorly understood.

As far as the basic mechanism is concerned, Indian monsoon has been proposed to be a manifestation of the giant land-sea breeze which originates due to the large land-sea temperature contrast between the Indian landmass and the adjacent oceanic region (Clemens et al. 1991; Webster et al. 1998). However, of late, the importance of latitudinal position of inter tropical convergence zone (ITCZ) in modulating the Indian monsoon has been realized. The switch from summer to winter monsoon is attributed to the shift in the position of inter-tropical convergence zone (ITCZ) from a more northerly position (15-25°N) during summer to a near equatorial or a low latitude southern hemispheric position (0-5° S) during winter (Fig. 1), which again is influenced by the change in SST of the Indian Ocean. A combination of both the heat lows due to land-sea temperature contrast, and latitudinal position of ITCZ are thought to be responsible for the rainfall in Indian subcontinent (Gadgil 2003, 2007).

According to Gadgil (2003), there are two favorable locations for ITCZ during summer in the Indian region, viz. one over the heated subcontinent and another over the warm waters of the equatorial Indian Ocean (Fig. 2). These two favorable zones have been termed as tropical convergence zones (TCZs, rather than the ITCZ), when referring to the Indian longitudes. It is observed that an abundant Indian summer rainfall (ISM) is an outcome of timely and periodic northward migration of cloud bands

concentrated over the oceanic TCZ (located in equatorial region) towards the continental TCZ (located in 15-25°N latitudinal zone). The migration of cloud bands from the oceanic TCZ to the continental TCZ depends on the temperature gradient between these two regions (Sikka and Gadgil 1980). Since the rainfall in the Indian summer monsoon zone has been shown to be facilitated by the northward movement of oceanic TCZ, convection over the equatorial Indian Ocean can be unfavorable as it may lead to a competition between the oceanic and continental TCZ (Gadgil et al. 2004). The periods of no rain, or breaks in the monsoon have been observed to occur during the development of low pressure system in the equatorial region, which retards the northward migration of cloud bands from equatorial region to the continental TCZ (Koteswaram 1950; Krishnan et al. 2000; RameshKumar et al. 2005; Rajeevan et al. 2008). Furthermore, it has been noted that the sea surface temperature (SST) of the adjacent seas affects the strength and the position of TCZs and thus the Indian monsoon (Gadgil 2003; Rao and Goswami 1988; Shukla 1975; He 2009). Further, Meehl (1997) showed that oceanic SST can control the inter-annual variation in the monsoon intensity by way of air-sea negative feedback mechanism.

Therefore, it is important to understand the link between the equatorial Indian Ocean SST and the Indian monsoon and compare such relationship with the changing latitudinal insolation contrast as it controls the latitudinal position and strength of TCZs. The long-term history of the temperature and monsoon spanning glacial-interglacial cycles can help understand this link between Indian Summer Monsoon (ISM), SST and seasonal latitudinal insolation gradient. Such records have been generated from a few parts of the Indian Ocean (Rostek et al. 1993; Dahl and Oppo 2006). More such studies are however required to rigorously understand the SST and monsoon relationship.

In the geologic past, a fairly good estimate of changes in the monsoon precipitation can be obtained by reconstructing changes in the seawater stable oxygen isotopic ratio from critical locations. The oxygen isotopic composition of the foraminiferal tests is mainly affected by temperature and oxygen isotopic composition of the seawater (Spero et al. 1997; Bemis et al. 1998). The oxygen isotopic composition of the seawater depends on both the global ice volume changes and local precipitation-evaporation and fresh water runoff. Thus by correcting the foraminiferal $\delta^{18}\text{O}$ record for continental ice volume (Shackleton 2000; Waelbroeck et al. 2002) and temperature changes, an estimate of past local seawater salinity changes can be obtained (Duplessy 1982; Weldeab et al. 2006, 2007a). With the development of technique of Mg/Ca-based SST estimate (Nurnberg et al. 1996; Lea 2000), paired

Mg/Ca and oxygen isotopic analysis of surface dwelling planktic foraminifera can therefore be used to reconstruct past sea surface salinity (Lea et al. 2000, 2006; Weldeab et al. 2006).

Here, we present ice-volume and temperature corrected surface seawater $\delta^{18}\text{O}$ ($\delta^{18}\text{O}_{\text{sw-icv}}$) reconstruction (a proxy for past seawater salinity and thus monsoon) over the last ~ 137 kyr, from the EIO, by using paired Mg/Ca and $\delta^{18}\text{O}$ of planktic foraminiferal species *Globigerinoides ruber* (white). The reconstructed $\delta^{18}\text{O}_{\text{sw-icv}}$ record has been compared with seasonal changes in low latitude insolation in the northern hemisphere over the past.

Oceanographic Setting

The study area lies in the EIO and the sea surface salinity in this region depends on evaporation-precipitation and freshwater runoff in both the Arabian Sea and Bay of Bengal (Shankar et al. 2002). The dry northeasterly winds along with winter cooling and evaporation, as well as large-scale precipitation, heating and freshwater discharge during the southwest monsoon season affect the large-scale seasonal surface circulation in northeastern Indian Ocean (Schott and McCreary 2001; Shankar et al. 2002). A basin-wide anti-cyclonic gyre, with East India Coastal Current (EICC) as its western boundary forms in the Bay of Bengal during February to May, and disappears during the summer monsoon (Schott and McCreary 2001) (Fig. 3). At the onset of the northeast monsoon season, the EICC flows southward from the Bengal shelf and meets the westward flowing northeast monsoon current (NMC) in the southern Bay of Bengal and transports 11 Sverdrup (Sv) ($1 \text{ Sv} = 10^6 \text{ m}^3/\text{s}$) of relatively less saline water from the Bay of Bengal to the eastern Arabian Sea (Schott et al. 1994). However, the southwards flowing EICC ceases rapidly during the height of the northeast monsoon season. During the inter-monsoon period in March, the EICC flows northward all along the east coast of India, and attains its maximum strength during April (Eigenheer and Quadfessel 2000). A strong southwest monsoon current (SMC) develops in the EIO during summer monsoon and transports 8.4 Sv water in to the Bay of Bengal. The region around southernmost tip of the western coast of India is characterized by an anti-cyclonic (cyclonic) gyre during winter (summer) monsoon and results in increased SSTs in this region. The presence of a gyre around southern tip of the western coast of India, shifts the monsoon currents away from the coast (Bruce et al. 1994). The core SK 157-04 lies under the influence of seasonal monsoon currents and the eastward equatorial jet (EEJ) (Hastenrath et al. 1993) which is driven by strong westerly winds during intermonsoon months (April-May and October-November).

The highest SST in the EIO is noted during spring season. During summer season, a band of warm water is located in the central EIO, while the region north and south of it remains relatively cool. The eastern EIO forms a part of the Indo-Pacific warm pool. In the EIO region, the highest SSS is noted in the western EIO, while the eastern EIO remains less saline during all seasons under the influence of the huge fresh water discharge into the Bay of Bengal (Levitus and Boyer, 1994).

The sea surface salinity decreases by ~ 1.5 psu during early winter season as compared to the previous month, indicating that the study area lies in the winter monsoon precipitation belt (Levitus and Boyer 1994; Goswami 2005). Above the core site, the lowest sea surface salinity (SSS) (33.55, monthly averaged) is reported during the month of November. The highest sea surface temperature (29.6°C) is reported during pre southwest monsoon season, while the lowest (28.0°C) during winter monsoon season (Levitus and Boyer 1994) (Fig. 4).

Materials and Methodology

A total of 132 samples from the top 270 cm section of a core (SK 157-04), collected from the eastern flank of the Comorin ridge in the equatorial Indian Ocean ($02^{\circ}40'\text{N}$, $78^{\circ}00'\text{E}$, water depth 3500 m) (Fig. 3) were used for the study. The Mg/Ca analysis was carried out on the surface dwelling planktic foraminiferal species *Globigerinoides ruber* (white) (250-355 μm size range). The procedure for cleaning the foraminiferal test included oxidative and reductive step (Martin and Lea 2002), the removal of silicate and pyrites grain under microscope, and centrifugation of sample immediately after weak acid dissolution and transfer into new acid cleaned vials (Greaves et al. 2005).

The chronology for the upper part of the core was established based on monospecific (*Globorotalia menardii*) Accelerator Mass Spectrometer (AMS) and conventional radiocarbon dates. The radiocarbon ages were calibrated to calendar years before present (1950) using calibration program (Calib Rev 5.0.2) of Stuiver and Reimer (1993). The chronology was extended down to 137 kyr by tuning the *G. ruber* $\delta^{18}\text{O}$ record to the low latitude isotope record of Bassinot et al (1994). The core top sample was dated as ~ 5 kyr old. The details of Mg/Ca analysis along with the chronology have been discussed by Saraswat et al (2005). For isotopic analysis of planktic foraminifera, 15-20 clean specimens of *Globigerinoides ruber* (white) from 250-355 μm size range were transferred to the glass vials. The stable isotopic ratio was measured at the Alfred Wegener Institute for Polar and Marine Research (Bremerhaven) using “Finnigan MAT 251 isotope ratio gas mass spectrometer” coupled to an automatic carbonate preparation device (Kiel I) and calibrated via NBS 19 to the PDB scale. The values are given

in δ -notation versus VPDB (Vienna Pee Dee Belemnite). Precision of oxygen isotope measurements based on repeat analyses of a laboratory standard over a one year period was better than 0.09‰.

Before calculating the $\delta^{18}\text{O}_{\text{sw}}$, in view of the in-equilibrium of $\delta^{18}\text{O}$ *G. ruber* with respect to the expected value, the $\delta^{18}\text{O}$ *G. ruber* values were corrected by a factor of 0.50‰ (Shackleton et al. 1973; Duplessy et al. 1981). The seawater oxygen isotopic composition was then calculated from the Mg/Ca based seawater temperature estimates and *G. ruber* $\delta^{18}\text{O}_{\text{cor}}$, by using the paleotemperature equation given by Kim and O'Neil (1997), which can be rewritten as

$$\delta^{18}\text{O}_{\text{seawater}} = \delta^{18}\text{O}_{\text{calcite}} + 0.27 - \frac{4.38 - \sqrt{4.38^2 - 4 \times 0.1 \times (16.9 - \text{Temp.})}}{2 \times 0.1}$$

The seawater oxygen isotopic composition was also estimated by using the equation given by Bemis et al (1998), yielding results very similar to those obtained using Kim and O'Neil (1997) equation. Based on the error estimates of analytical reproducibility of SSTs based on triplicate analyses of samples and $\delta^{18}\text{O}_{\text{c}}$, an overall error estimate (1σ) for reconstructed $\delta^{18}\text{O}_{\text{sw}}$ is $\pm 0.13\text{‰}$. The contribution of continental ice volume changes, as estimated by Waelbroeck et al (2002), was removed from the seawater oxygen isotopic composition to estimate the local seawater oxygen isotopic composition ($\delta^{18}\text{O}_{\text{sw-ivc}}$).

The change in $\delta^{18}\text{O}_{\text{sw-ivc}}$ relative to the present day value ($\Delta\delta^{18}\text{O}_{\text{sw-ivc}}$) was then calculated by subtracting the modern surface seawater oxygen isotopic composition (0.32) as measured near the core location by Bouvier-Soumagnac and Duplessy (1985). However, such an estimate of variation in local seawater isotopic composition with respect to present should be seen in context of the potential uncertainty due to snap-shot seawater oxygen isotopic measurements, which may differ from the annual average oxygen isotopic composition of seawater at the location. The residual $\delta^{18}\text{O}_{\text{sw-ivc}}$ indicates the local precipitation-evaporation changes.

The conversion of local seawater oxygen isotopic changes into salinity depends on the precise estimation of relationship between seawater salinity and oxygen isotopic composition. Here we have established the relationship between $\delta^{18}\text{O}_{\text{sw}}$ and salinity based on 117 points in the EIO (10°S-10°N, 50°E-100°E) downloaded from Global Seawater Oxygen-18 Database of the Goddard Institute for Space Studies (Schmidt et al. 1999). The salinity obtained by using core top Mg/Ca SST, $\delta^{18}\text{O}_{\text{sw}}$ and $\delta^{18}\text{O}_{\text{sw-SSS}}$ relationship deduced from the modern measurement (Fig. 5), match very well with the Levitus

annual SSS over the core site, showing values of 34.7 and 34.8, respectively. Delaygue et al (2001) also developed a seawater oxygen isotope/salinity relationship for the Bay of Bengal based on the oxygen isotopic composition of the seawater, and the same has also been used to calculate the paleosalinity in the present study. Though estimation of seawater salinity from the coupled stable oxygen isotopic composition and Mg/Ca ratio of the foraminifera may involve errors due to uncertain $\delta^{18}\text{O}_{\text{sw}}$ and salinity relationship (Schmidt 1999, Rohling 2007), this is the only available technique (except Ba/Ca ratio of foraminifera, which works well at locations off large river system (Weldeab et al. 2007a, Weldeab et al. 2007b)) to reconstruct past salinity changes from the open ocean and has been widely used in the northern Indian Ocean (Govil and Naidu 2010; Banakar et al. 2010).

The winter, represented by the month January, and summer (July) seasonal insolation at the equator and different northern latitudes (5°N , 10°N , 15°N , 20°N , 25°N) for the last 150 kyr, was taken from Laskar et al (2004). This latitudinal zone was chosen as it is the zone of monsoon buildup and precipitation in the Indian subcontinent (Gadgil 2003). The seasonal latitudinal anomaly was calculated by subtracting the insolation value at the equator from the value at respective latitudes during particular season and time.

Results

The core top Mg/Ca SST (28.1°C) matches well with the modern SST (28.5°C) (Levitus and Boyer, 1994) over the core location and also with the core top Mg/Ca SST values (28.5°C) calculated at another nearby site MD 90-0963 (Tachikawa et al. 2008) (Fig. 6). The core top $\delta^{18}\text{O}$ *G. ruber* (-1.93‰) is depleted than that of the *G. ruber* collected in plankton tows (-2.69‰) from a station south of the present site (Shackleton et al. 1973) and also from the core top $\delta^{18}\text{O}$ *G. ruber* of MD 90-0963 (Tachikawa et al. 2008). The down core Mg/Ca SST variation shows that the EIO was $\sim 2.1^{\circ}\text{C}$ cooler during the Last Glacial Maximum (LGM) as compared to the present. The maximum SST during the penultimate interglacial period (stage 5e) was higher (29.9°C) than the maximum SST during the present interglacial period (28.8°C). The calculated core top $\delta^{18}\text{O}_{\text{sw}}$ (0.38) matches very well with the modern seawater oxygen isotopic composition (0.32) as measured near the core location by Bouvier-Soumagnac and Duplessy (1985).

The $\delta^{18}\text{O}_{\text{sw-ivc}}$ shows a systematically depleting trend during the last ~ 137 kyr BP. The local precipitation-evaporation and fresh water runoff induced changes made the seawater oxygen isotopic composition in the equatorial Indian Ocean most enriched during the later part of the oxygen isotopic

stage 6 and early part of the oxygen isotopic stage 5. The most depleted $\delta^{18}\text{Osw-ivc}$ values in the equatorial Indian Ocean during the last ~ 137 kyr are observed during the middle of the isotopic stage 2 and during the termination of isotopic stage 5 (Fig. 7).

A $\sim 0.7\text{‰}$ shift in $\delta^{18}\text{Osw-ivc}$ is noted during both the penultimate and last glacial-interglacial transitions (Fig. 7). Other major $\delta^{18}\text{Osw-ivc}$ variation ($\sim 0.7\text{‰}$ as compared to core top $\delta^{18}\text{Osw}$) is observed during isotopic stage 4. The $\delta^{18}\text{Osw-ivc}$ was more enriched during the peak last interglacial (Isotopic stage 5e) as compared to the peak present interglacial. During the onset and termination of isotopic stage 5, the $\delta^{18}\text{Osw-ivc}$ was relatively low. However during middle of the isotopic stage 5, the $\delta^{18}\text{Osw-ivc}$ was depleted. The seawater oxygen isotopic composition was $\sim 0.6\text{‰}$ lighter during the larger part of isotopic stage 4 as compared to the core top. During isotopic stage 3, the $\delta^{18}\text{Osw-ivc}$ shows an enriching trend till the beginning of isotopic stage 2.

The conversion of $\delta^{18}\text{Osw-ivc}$ into absolute salinity as discussed above shows that the sea surface salinity (SSS) in the EIO was higher than that at present only during 131-113 kyr BP (penultimate interglacial), 62-58 kyr BP and 24-30 kyr BP (Fig. 8). During rest of the ~ 137 kyr BP, salinity in the equatorial Indian Ocean region was lower than the modern sea surface salinity. The lowest salinity (upto $\sim 3.0\text{‰}$ lower) than at present is inferred during the last glacial maximum, while the highest salinity is reported during the penultimate glacial-interglacial transition, especially during the marine isotopic stage 5e. During the later part of the oxygen isotopic stage 5, SSS was lower by as much as $\sim 2.3\text{‰}$ decreasing sharply towards the isotopic stage 5/4 transition, only to increase equally rapidly (reaching upto $\sim 0.6\text{‰}$ higher than at present) during the isotopic stage 4. The SSS was higher than that at present during the MIS 4. During MIS4/3 transition, SSS again decreased sharply to a low of $\sim 1.7\text{‰}$, only to increase by $\sim 1.0\text{‰}$, before again decreasing by $\sim 1.8\text{‰}$ at 48 kyr BP. During the later part of the MIS3, SSS was higher than that present (0.4‰). During early part of the isotopic stage 3, salinity was comparable with that at present but increased to ~ 2.0 psu higher than that at present towards the isotopic stage 3/2 transition. The SSS increased sharply during the middle of termination 1, but was still lower than that present. From ~ 9 kyr BP onwards the salinity increased till present, with minor fluctuation in-between.

The comparison of salinity changes at EIO with the variation in latitudinal insolation gradient in the northern hemisphere during the last 137 kyr shows a peculiar relationship (Fig. 9). During the MIS, 2, 3 and 4, January insolation anomalies are significantly positively correlated (0.6) with EIO salinities

(Fig. 10). There is however, no correlation between July insolation anomaly and EIO salinities during the same period.

Discussion

In the modern conditions sea surface salinity decreases by ~ 1.5 psu due to the winter monsoon rains and transport of low salinity water from the eastern EIO to the central EIO by the winter monsoon currents (Schott and McCreary 2001). During summer season SST decreases by $\sim 1^\circ\text{C}$ and SSS slightly decreases by ~ 0.3 psu due to wind induced cooling and evaporation. On the basis of the assumption that the modern relationship of SSS changes in the EIO and seasonal wind field and fresh water input hold for the investigated time interval as well, we discuss changes in the $\delta^{18}\text{O}_{\text{sw-ivc}}$ record in the context of variation in the summer monsoon wind strength and winter monsoon precipitation in the equatorial region. Because equator and low northern tropical latitudes are mainly responsible for the Indian monsoon (Gadgil 2003), we investigate the relationship between seasonal latitudinal insolation gradient and the $\delta^{18}\text{O}_{\text{sw-ivc}}$ record to infer mechanisms for past changes in monsoon intensity in this region.

Throughout the last glacial period, decrease in sea surface salinity at the core site as compared to present, coincides with decreased insolation gradient between northern tropical latitudes and the equator during January (Fig. 9). We propose that this decreased insolation gradient during January might have affected the incursion of moisture from the oceanic TCZ towards the continental TCZ during summer by decreasing the build up of heat during pre-summer monsoon months in the northern tropical latitudes (Vernekar et al. 1995). The decreased heat buildup in the northern tropical latitudes prior to the summer monsoon season will result in weaker continental TCZ and reduced low tropospheric winds. The low tropospheric wind strength will decrease the moisture availability, which is an important component of monsoon. It is further supported by the observations that the seasonal latitudinal position of the surface trough or the zone responsible for monsoon lags the latitude of solar insolation by a couple of months (Gadgil 2007). Rao and Goswami (1988) and Clark et al (2000) also noted a strong positive correlation (0.87) between winter SST in the central Indian Ocean and rainfall in the Indian subcontinent. Thus the decreased January insolation gradient in the northern tropical latitudes would have weakened the strength of the continental TCZ. The weakened continental TCZ would have increased the competition between the oceanic and continental TCZs and thus less migration of the cloud bands from the oceanic TCZ towards the continental TCZ during summer monsoon season. The relatively decreased migration of the cloud bands from the oceanic TCZ towards the continental TCZ would have decreased the

summer monsoon strength. Similar views regarding more strong oceanic TCZ and weak continental TCZ being unfavorable for summer monsoon were suggested by Sikka and Gadgil (1980), Gadgil (2003) and Gadgil et al (2004). It is further supported by the presence of prominent equatorial TCZ during the breaks in summer monsoon (Koteswaram 1950, Krishnan et al. 2000).

Another implication of weakened continental TCZ is that the ITCZ might have been located in more southerly position during the last glacial period as compared to present. Therefore, the decreased summer monsoon strength is also attributed to the more southerly position of the ITCZ (more towards equator) during the last glacial period. The decreased summer monsoon strength due to more southerly location of the ITCZ during glacial times has also been reported from other parts of the world (Haug et al. 2001; Weldeab et al. 2006; Flietman et al. 2007; Weldeab et al. 2007a, Yancheva et al. 2007).

The decreased southwest monsoon strength in the Indian Ocean during the last glacial period has been reported in previous studies (Cullen 1981; Duplessy 1982; Fontugne and Duplessy 1986; Niitsuma et al. 1991; Prell and Kutzbach 1992; Nigam and Khare 1995; 1999; Naidu and Malmgren 1996; Anderson et al. 2002; Banakar et al. 2005; Anand et al. 2008). Earlier, it has been suggested that increased ice-sheets during glacial periods were a crucial factor in modulating monsoon changes (Chakraborty et al. 2002; Gupta and Thomas 2003, Gupta et al. 2004). However, here we propose that changes in seasonal latitudinal gradient were also equally crucial in shaping the intensity and areal extent of monsoon.

During the last 137 kyr BP, increased SSS in the EIO coincides with increased January insolation gradient in the northern tropical latitudes. It is attributed to strong continental TCZ leading to increased migration of cloud bands from oceanic TCZ towards continental TCZ and thus strengthened summer monsoon. However, not all the positive January insolation anomalies result in increased southwest monsoon strength. It can be attributed to the in-phase or out of phase effect of July insolation gradient, which may partially contribute to the heat buildup. But the contribution from the July insolation gradient in the northern tropical latitudes will be less due to its small amplitude as compared to the January insolation anomalies.

However, it should be noted that not all of the changes in salinity in the study area can be attributed to the changes in seasonal insolation gradient in the northern tropical latitudes, which is obvious due to the complex nature of processes leading to monsoon in the Indian subcontinent. A part of the changes in the monsoon intensity can also arise due to changing thermal structure of the Indo-Pacific

warm pool during the last glacial-interglacial period (Saraswat et al. 2007). A warmer eastern equatorial Pacific will result in decreased summer monsoon strength in the Indian subcontinent through decreased meridional gradient of tropospheric temperature over the south Asian monsoon region and thus shortening the length of rainy season (Goswami and Xavier 2005).

The increased winter monsoon precipitation during shift of continental TCZ towards more southerly latitudes is assigned to the increased availability of moisture for the easterly winds during winter monsoon. With a more southerly ITCZ, easterly winds will travel all over the Bay of Bengal to pick up increased amount of moisture and will ultimately result in enhanced precipitation during winter monsoon. Such changes in monsoon related processes like productivity due to changing insolation have also been studied by Beaufort et al (1997) from the EIO. Additionally, a more strong winter monsoon will lead to enhanced transport of low saline, cool waters from the eastern EIO to the western EIO by winter monsoon and equatorial currents. It will result in cooling in the western Arabian Sea, which is further detrimental for the summer monsoon (Shukla 1975). Recently Gadgil et al (2004) also noted that the eastern and western equatorial Indian Ocean SST is an important factor in regulating the Indian summer monsoon. The significantly reduced salinity during the last glacial maximum at this core site is thus assigned to increased winter monsoon strength.

The systematically depleting $\delta^{18}\text{O}_{\text{sw}}$ -I trend during the last ~137 kyr BP, though with the slope of the regression line being very small (~0.0023), might be part of a longer regional cycle. Similar observations were made by Lea et al (2000) from the $\delta^{18}\text{O}_{\text{sw}}$ variations over the late Quaternary in the cores collected from the equatorial Pacific Ocean.

A comparison of Mg/Ca-based estimates of seawater temperature (Saraswat et al. 2005) with the salinity, shows that a minor change in the seawater temperature leads to a significant change in the seawater salinity which in turn reflects a large-scale variation in the intensity and duration of monsoon in the Indian subcontinent and adjacent areas.

Conclusions

Based on the paired stable oxygen and Mg/Ca analysis on planktic foraminiferal species *G. ruber* from a core collected from the EIO, covering the last ~137 kyr, we show that during the last two glacial-interglacial transitions, the $\delta^{18}\text{O}_{\text{sw}}$ changed by ~1.4‰. The study indicates that the $\delta^{18}\text{O}_{\text{sw}}$ -based estimate of SSS was lower than that at present almost throughout the last glacial period. Higher than modern SSS, is reported only during 131-113 kyr BP (penultimate interglacial), 62-58 kyr BP and 24-30

kyr BP. The highest salinity as compared to present is inferred during the penultimate glacial-interglacial transition. A comparison of the seasonal latitudinal insolation gradient in the northern hemisphere, shows that the January insolation anomaly at northern latitudes has a significant correlation (0.6) with the $\delta^{18}\text{O}_{\text{sw-ivc}}$ during the MIS 2, 3 and 4. The positive January insolation anomaly at northern latitudes coincides with increased $\delta^{18}\text{O}_{\text{sw-ivc}}$. Such high salinity episodes are inferred as indicators of strong summer monsoon events that result in high wind intensity, increased evaporation and thus higher salinity in the study area. Rest of the period is inferred as strengthened northeast monsoon and weaker summer monsoon intervals as the core site lies in the winter monsoon precipitation belt. Based on the relationship between January insolation anomaly at northern latitudes and salinity changes from the study area we infer that the southwest monsoon was stronger than that at present during 131-113 kyr BP (penultimate interglacial), 62-58 kyr BP and 24-30 kyr BP. The summer monsoon system was weaker during rest of the last ~137 kyr period, whereas winter monsoon was stronger during rest of the last ~137 kyr. The study shows that winter time insolation difference between northern latitudes and equator exerts a strong control on the Indian monsoon strength during the glacial period.

Acknowledgements

Authors are thankful to the Director, National Institute of Oceanography, for the encouragement and permission to publish the findings. The manuscript has greatly improved with the comments and suggestions of Drs. P.D. Naidu and V.K. Banakar of the National Institute of Oceanography, India. The help from the staff at Alfred Wegner Institute for Polar and Marine Research, Germany during stable isotopic analysis is thankfully acknowledged. One of authors (RS) is thankful to the Indo-US Science and Technology Forum and Council of Scientific and Industrial Research, India for providing financial support.

References:

- Anand P, Kroon D, Singh, AD, Ganeshram RS, Ganssen G, Elderfield H (2008) Coupled sea surface temperature–seawater $\delta^{18}\text{O}$ reconstructions in the Arabian Sea at the millennial scale for the last 35 ka. *Paleoceanography* 23:PA4207, doi:10.1029/2007PA001564.
- Anderson DM, Overpeck JT, Gupta AK (2002) Increase in the Asian southwest monsoon during the past four centuries. *Science* 297:596-599.
- Banakar VK, Oba T, Chodankar AR, Kuramoto T, Yamamoto M, Minagawa M (2005) Monsoon related changes in sea surface productivity and water column denitrification in the Eastern Arabian Sea during the last glacial cycle. *Mar Geol* 219:99-108.
- Banakar VK, Mahesh BS, Burr G, Chodankar AR (2010) Climatology of the Eastern Arabian Sea during the last glacial cycle reconstructed from paired measurement of foraminiferal $\delta^{18}\text{O}$ and Mg/Ca. *Quat Res* 73:535-540.
- Bassinot FC, Labeyrie LD, Vincent EXQ, Shackleton NJ, Lancelot Y (1994) The astronomical theory of climate and the age of the Brunhes-Matuyama magnetic reversal. *Earth Planet Sci Lett* 126:91-108.
- Beaufort L, Lancelot Y, Camberlin P, Cayre O, Vincent E, Bassinot F, Labeyrie L (1997) Insolation cycles as a major control of equatorial Indian Ocean primary production. *Science* 278:1451-1454.
- Bemis BE, Spero HJ, Bijma J, Lea DW (1998) Reevaluation of the oxygen isotopic composition of planktonic foraminifera: experiment results and revised paleotemperature equations. *Paleoceanography* 13:150-160.
- Bouvier-Soumagnac Y, Duplessy JC (1985) Carbon and oxygen isotopic composition of planktonic foraminifera from laboratory culture, plankton tows and Recent sediment; implications for the reconstruction of paleoclimatic conditions and of the global carbon cycle. *J Foramin Res* 15:302-320.
- Bruce JG, Johnson DR, Kindle JC (1994) Evidence for eddy formation in the eastern Arabian Sea during the northeast monsoon. *J Geophys Res* 99:7651-7664.
- Chakraborty A, Nanjundiah RS, Srinivasan J (2002) Role of Asian and African orography in Indian summer monsoon. *Geophys Res Lett* 29:10.1029/2002GL015522, 1-4.
- Clark CO, Cole JE, Webster PJ (2000) Indian Ocean SST and Indian summer rainfall: Predictive relationships and their decadal variability. *J Clim* 13:2503-2519.
- Clemens SC, Prell WL, Murray DW, Shimmield G, Weedon G (1991) Forcing mechanisms of the Indian Ocean monsoon. *Nature* 353:720-725.
- Cullen JL (1981) Microfossil evidence for changing salinity patterns in the Bay of Bengal over the last 20000 years. *Palaeogeogra Palaeoclimatol Palaeoecol* 35:315-356.
- Dahl KA, Oppo DW (2006) Sea surface temperature pattern reconstructions in the Arabian Sea. *Paleoceanography* 21:PA1014, doi:10.1029/2005PA001162.

- Delaygue G, Bard E, Rollion C, Jouzel J, Stiévenard M, Duplessy JC, Ganssen G (2001) Oxygen isotope/salinity relationship in the northern Indian Ocean. *J Geophys Res* 106: 4565-4574.
- Duplessy JC, Blanc PL, Bé AWH (1981) Oxygen-18 enrichment of planktonic foraminifera due to gametogenic calcification below the euphotic zone. *Science* 213:1247-1250.
- Duplessy JC (1982) Glacial to interglacial contrasts in the northern Indian Ocean. *Nature* 295:494-498.
- Eigenheer A, Quadfasel D (2000) Seasonal variability of the Bay of Bengal circulation inferred from TOPEX/Poseidon altimetry. *J Geophys Res* 105:3243-3252.
- Fleitmann D, Burns SJ, Mangini A, Mudelsee M, Kramers J, Villa I, Neff U, Al-Subbary AA, Buettner A, Hippler D, Matter A (2007) Holocene ITCZ and Indian monsoon dynamics recorded in stalagmites from Oman and Yemen (Socotra). *Quat Sci Rev* 26: 170-188.
- Fontugne MR, Duplessy JC (1986) Variations of the monsoon regime during the upper quaternary: Evidence from carbon isotopic record of organic matter in North Indian Ocean sediment cores. *Palaeogeogra Palaeoclimatol Palaeoecol* 56:69-88.
- Gadgil S (2003) The Indian monsoon and its variability. *Annu Rev Earth Planet Sci* 31:429-467.
- Gadgil S, Vinayachandran PN, Francis PA, Gadgil S (2004) Extremes of the Indian summer monsoon rainfall, ENSO and equatorial Indian Ocean oscillation. *Geophys Res Lett* 31: L12213, doi:10.1029/2004GL019733.
- Gadgil S (2007) The Indian monsoon 3: Physics of the monsoon *Resonance* 12:4-20.
- Goswami BN (2005) South Asian Summer Monsoon: An overview: in *The Global Monsoon System: Research and Forecast*. Edited by C.-P. Chang, Bin Wang, Ngar-Cheung Gabriel Lau 5: 47-71.
- Goswami BN, Xavier PK (2005) ENSO control on the south Asian monsoon through the length of the rainy season. *Geophys Res Lett* 32: L18717, doi:10.1029/2005GL023216.
- Govil P, Naidu PD (2010) Evaporation-precipitation changes in the eastern Arabian Sea for the last 68 ka: Implications on monsoon variability. *Paleoceanography* 25:PA1210, doi:10.1029/2008PA001687.
- Greaves M, Barker S, Daunt C, Elderfield H (2005) Accuracy, standardisation and interlaboratory calibration standards for foraminiferal Mg/Ca thermometry. *Geochem Geophys Geosyst* 6: doi:10.1029/2004GC000790.
- Gupta AK, Thomas E (2003) Initiation of Northern Hemisphere glaciation and strengthening of the northeast Indian monsoon: Ocean Drilling Program Site 758, eastern equatorial Indian Ocean. *Geology* 31:47-50.
- Gupta AK, Singh RK, Joseph S, Thomas E (2004) Indian Ocean high-productivity event (10-8 Ma): linked to global cooling or to the initiation of the Indian monsoons?. *Geology* 32:753-756.
- Hastenrath S, Nicklis A, Greischar L (1993) Atmospheric-hydrospheric mechanisms of climate anomalies in the western equatorial Indian Ocean. *J Geophys Res* 98:20219-20235.

- Haug GH, Hughen KA, Sigman DM, Peterson LC, Rohl U (2001) Southward migration of the Intertropical Convergence Zone through the Holocene. *Science* 293:1304-1308.
- He JH (2009) A review of Asian-Pacific monsoon. *Atmos Oceanic Sci Lett* 2:91-96.
- Kim ST, O'Neil JR (1997) Equilibrium and nonequilibrium oxygen isotope effects in synthetic carbonates. *Geochim Cosmochim Acta* 61:3461-3475.
- Koteswaram P (1950) Upper air lows in low latitudes in the Indian area during southwest monsoon season and "Breaks" in the monsoon. *Ind J Met Geophys* 1:162-64.
- Krishnan R, Zhang C, Sugi M (2000) Dynamics of breaks in the Indian summer monsoon. *J Atmos Sci* 57:1354-1372.
- Laskar J, Robutel P, Joutel F, Gastineau M, Correia ACM, Levrard B (2004) A long term numerical solution for the insolation quantities of the Earth. *Astron & Astrophys* 428: 261-285.
- Lea DW, Pak DK, Spero HJ (2000) Climate impact of late Quaternary equatorial Pacific sea surface temperature variations. *Science* 289:1719-1724.
- Lea DW, Pak DK, Belanger CL, Spero HJ, Hall MA, Shackleton NJ (2006) Paleoclimate history of Galápagos surface waters over the last 135,000 years. *Quat Sci Rev* 25:1152-1167.
- Levitus S, Boyer T (1994) *World Ocean Atlas 1994, vol. 4, Temperature*, NOAA Atlas NESDIS 4, U.S. Dept of Commer Washington, D.C.
- Martin PA, Lea DW (2002) A simple evaluation of cleaning procedures on fossil benthic foraminiferal Mg/Ca. *Geochem Geophys Geosyst* 3:8401, doi:10.1029/2001GC000280.
- Meehl GA (1997) The south Asian monsoon and the tropospheric biennial oscillation. *J Clim* 10:1921-1943.
- Molnar P, England P, Martiod J (1993) Mantle dynamics, uplift of the Tibetan Plateau and the Indian monsoon development. *Rev Geophys* 34:357-396.
- Naidu PD, Malmgren BA (1996) A high-resolution record of late Quaternary upwelling along the Oman Margin Arabian Sea based on planktonic foraminifera. *Paleoceanography* 11:129-140.
- Nigam R, Khare N (1995) Significance of correspondence between river discharge and proloculus size of benthic foraminifera in paleomonsoonal studies. *Geo-Mar Lett* 15:45-50.
- Nigam R, Khare N (1999) Spatial and temporal distribution of foraminifera in sediments off the central west coast of India and use of their test morphologies for the reconstruction of palaeomonsoonal precipitation. *Micropaleontology* 45:1-15.
- Niitsuma N, Oba T, Okada M (1991) Oxygen and carbon isotope stratigraphy at site 729, Oman margin. *Proc ODP Sci Results* 117:321-341.
- Nurnberg D, Bijma J, Hemleben C (1996) Assessing the reliability of magnesium in foraminiferal calcite as a proxy for water mass temperatures. *Geochim Cosmochim Acta* 60:803-814.

- Prell WL, Kutzbach JE (1992) Sensitivity of the Indian monsoon to forcing parameters and implications for its evolution. *Nature* 360:647-652.
- Prell WL, Kutzbach JE (1997) The impact of Tibet-Himalaya elevation on the sensitivity of the monsoon climate system to changes in solar radiation, in Ruddiman, W.F., ed., *Tectonic uplift and climate change*: New York, Plenum Press. 172-203.
- Rajeevan M, Gadgil S, Bhate J (2008) Active and break spells of the Indian summer monsoon. Research Report, National Climate Center, India Meteorological Department, Pune.
- RameshKumar MR, Shenoi SSC, Schultz J (2005) Impact of convection over the equatorial trough on summer monsoon activity over India. *Int J Remote Sens* 26:4747-4762.
- Rao KG, Goswami BN (1988) Interannual variations of sea surface temperature over the Arabian Sea and the Indian monsoon: A new perspective. *Month Weath Rev* 116:558-568.
- Rohling EJ (2007) Progress in paleosalinity: Overview and presentation of a new approach. *Paleoceanography* 22:PA3215, doi:10.1029/2007PA001437.
- Rostek F, Ruhland G, Bassinot F, Muller PJ, Labeyrie L, Lancelot Y, Bard E (1993) Reconstructing sea surface temperature and salinity using $\delta^{18}\text{O}$ and alkenone records. *Nature* 364:319-321.
- Saraswat R, Nigam R, Weldeab S, Mackensen A, Naidu PD (2005) A first look at past sea surface temperatures in the equatorial Indian Ocean from Mg/Ca in foraminifera. *Geophys Res Lett* 32:L24605, doi:10.1029/2005GL024093.
- Saraswat R, Nigam R, Weldeab S, Mackensen A (2007) The tropical warm pool in the Indian Ocean and its influence on ENSO over the past 137,000 yr BP. *Curr Sci* 92:1153-1156.
- Schmidt GA (1999) Error analysis of paleosalinity calculations. *Paleoceanography* 14:422-429.
- Schmidt GA, Bigg GR, Rohling EJ (1999) "Global Seawater Oxygen-18 Database". <http://data.giss.nasa.gov/o18data/>.
- Schott FA, Reppin J, Fischer J, Quadfasel D (1994) Currents and transports of the Monsoon Current south of Sri Lanka. *J Geophys Res* 99:25127-25141.
- Schott FA, McCreary JP Jr (2001) The monsoon circulation of the Indian Ocean. *Prog Oceanogra* 51:1-123.
- Shackleton NJ, Wiseman JDH, Buckley HA (1973) Non-equilibrium isotopic fractionation between seawater and planktonic foraminiferal tests. *Nature* 242:177-179.
- Shackleton NJ (2000) The 100,000-year ice-age cycle identified and found to lag temperature, carbon dioxide, and orbital eccentricity. *Science* 289:1897-1902.
- Shankar D, Vinayachandran PN, Unnikrishnan AS (2002) The monsoon currents in the north Indian Ocean. *Prog Oceanogra* 52:63-120.
- Shukla J (1975) Effect of Arabian Sea surface temperature anomaly on Indian summer monsoon: A numerical experiment with the GFDL model. *J Atmos Sci* 32:503-511.

- Sikka OR, Gadgil S (1980) On the maximum cloud zone and the ITCZ over Indian longitudes during the South west monsoon. *Mon Weather Rev* 108:1840-1853.
- Spero HJ, Bijma J, Lea DW, Bemis BE (1997) Effect of seawater carbonate concentration on foraminiferal carbon and oxygen isotopes. *Nature* 390:497-500.
- Stuiver M, Reimer PJ (1993) Extended ¹⁴C data base and revised CALIB 3.0 ¹⁴C age calibration program. *Radiocarbon* 35:15-230.
- Tachikawa K, Sepulcre S, Toyofuku T, Bard E (2008) Assessing influence of diagenetic carbonate dissolution on planktonic foraminiferal Mg/Ca in the southeastern Arabian Sea over the past 450 ka: Comparison between *Globigerinoides ruber* and *Globigerinoides sacculifer*. *Geochem Geophys Geosyst* 9:Q04037, doi:10.1029/2007GC001904.
- Tiwari M, Ramesh R, Somayajulu BLK, Jull AJT, Burr GS (2005) Early deglacial (19-17 ka) strengthening of the northeast monsoon. *Geophys Res Lett* 32:L19712, doi:10.1029/2005GL024070.
- Vernekar AD, Zhou J, Shukla J (1995) The effect of Eurasian snow cover on the Indian monsoon. *J Clim* 8:248-266.
- Waelbroeck C, Labeyrie L, Michel E, Duplessy JC, McManus JF, Lambeck K, Balbon E, Labracherie M (2002) Sea-level and deep water temperature changes derived from benthic foraminifera isotopic records. *Quat Sci Rev* 21: 295-305.
- Webster PJ, Magafia VO, Palmer TN, Shukla J, Tomas RA, Yanai M, Yasunari T (1998) Monsoons: Processes, predictability, and the prospects for prediction. *J Geophys Res* 103:14,451-14,510.
- Weldeab S, Schneider RR, Kolling M (2006) Deglacial sea surface temperature and salinity increase in the western tropical Atlantic in synchrony with high latitude climate instabilities. *Earth Planet Sci Lett* 241:699-706.
- Weldeab S, Lea DW, Schneider RR, Andersen N (2007a) 155,000 years of West African monsoon and ocean thermal evolution. *Science* 316:1303-1307.
- Weldeab S, Lea DW, Schneider RR, Andersen N (2007b) Centennial scale climate instabilities in a wet early Holocene West African monsoon. *Geophys Res Lett* 34: L24702, doi:10.1029/2007GL031898.
- Yancheva G, Nowaczyk NR, Mingram J, Dulski P, Schettler G, Negendank JFW, Liu J, Sigman DM, Peterson LC, Haug GH (2007) Influence of the intertropical convergence zone on the east Asian monsoon. *Nature* 445:74-77.

Legend to Figures:

- Figure 1: The latitudinal position of the Inter-tropical convergence zones (ITCZ) during summer (July) and winter (January) in the Indian subcontinent. Note that the ITCZ shift in the southern hemisphere during the winter is very less with respect to the equator as compared to that in the northern hemisphere during the summer (Modified after Gadgil 2003, 2007).
- Figure 2: The latitudinal position of the oceanic and continental tropical convergence zones (TCZs) along 80°E longitude during July and August. Both the TCZs develop in the beginning of summer monsoon and are present throughout the summer monsoon months (Modified after Gadgil 2003).
- Figure 3: Location of the core and the major surface circulation features in the study area. A. Winter monsoon circulation, B. Summer monsoon circulation (EC- Equatorial Current; SECC- South equatorial counter current; LH- Lakshadweep High; LL- Lakshadweep Low; WICC- West India Coastal Current; EICC- East India Coastal Current; SMC- Summer Monsoon Current; NMC- Northeast (Winter) Monsoon Current) (Modified after Schott and McCreary 2001).
- Figure 4: Monthly sea surface temperature and salinity at the core site (Levitus and Boyer 1994).
- Figure 5: The relationship between $\delta^{18}\text{O}_{\text{sw}}$ and salinity based on 117 points in the EIO (10°S-10°N latitude, 50°E-100°E longitude) downloaded from Global Seawater Oxygen-18 Database of the Goddard Institute for Space Studies (Schmidt et al. 1999).
- Figure 6: Temporal variation in the sea surface temperature and $\delta^{18}\text{O}$ *G. ruber* over the last ~137 kyr BP in the equatorial Indian Ocean.
- Figure 7: Temporal variation in the seawater oxygen isotopic composition over the last ~137 kyr BP in the equatorial Indian Ocean. The horizontal line shows the modern seawater oxygen isotope composition.
- Figure 8: The salinity changes as compared to present over the last ~137 kyr BP in the equatorial Indian Ocean based on the relationship established on the basis of modern $\delta^{18}\text{O}_{\text{sw}}$ and salinity measurements and the equation given by Delague et al (2001). Both of the equations provide a similar salinity estimate. The horizontal line shows the annual average sea surface salinity.
- Figure 9: The plot shows salinity changes as compared to present, reconstructed sea surface temperature in the equatorial Indian Ocean and seasonal insolation gradient in the tropical northern latitudes with respect to the equator.
- Figure 10: Relationship between January insolation gradient in the tropical northern latitudes and the salinity changes in the equatorial Indian Ocean during the MIS 2, 3 and 4.

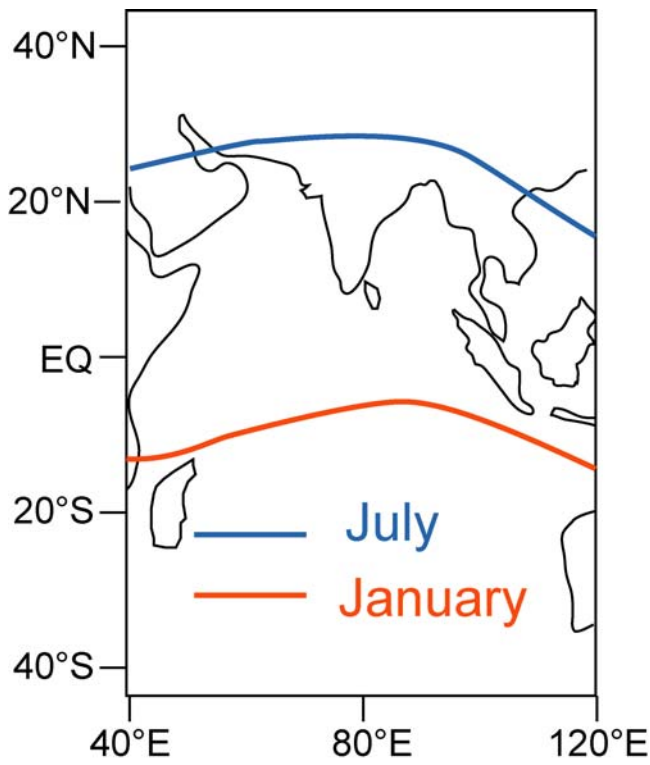


Figure 1

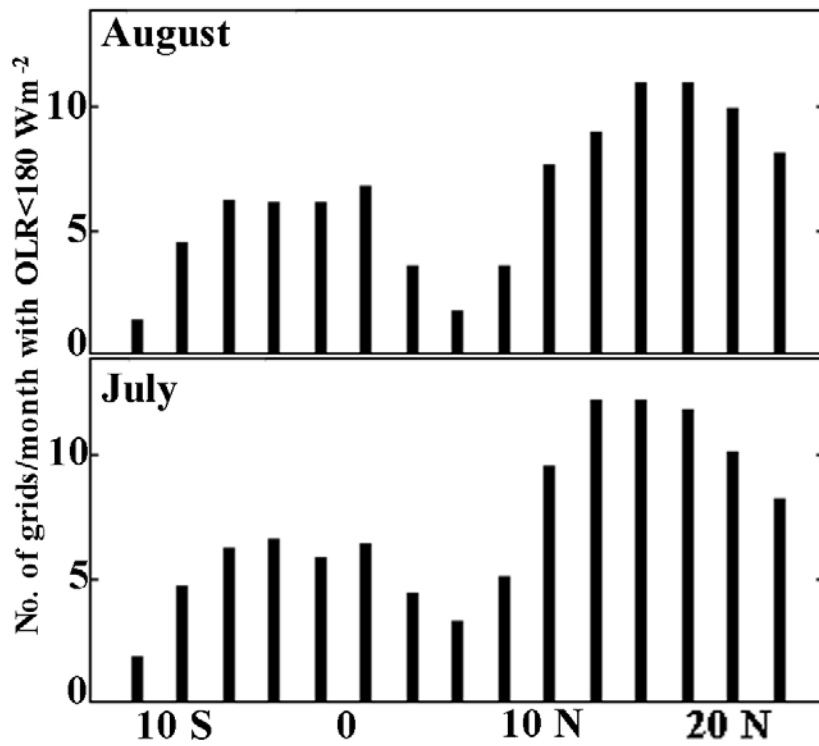


Figure 2

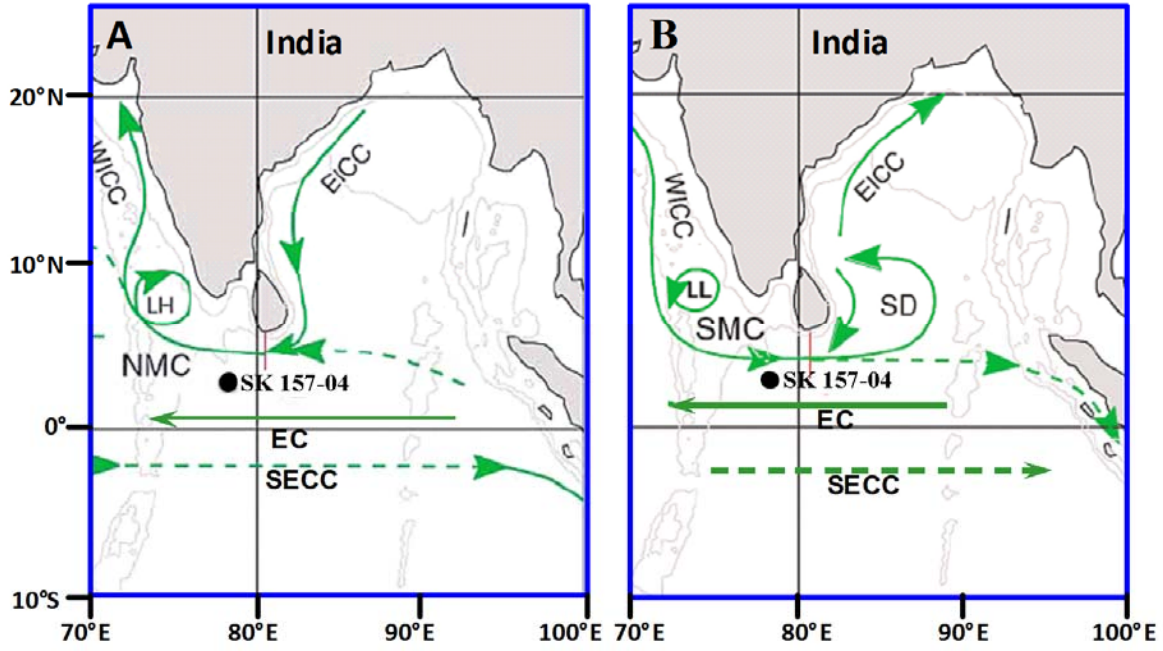


Figure 3

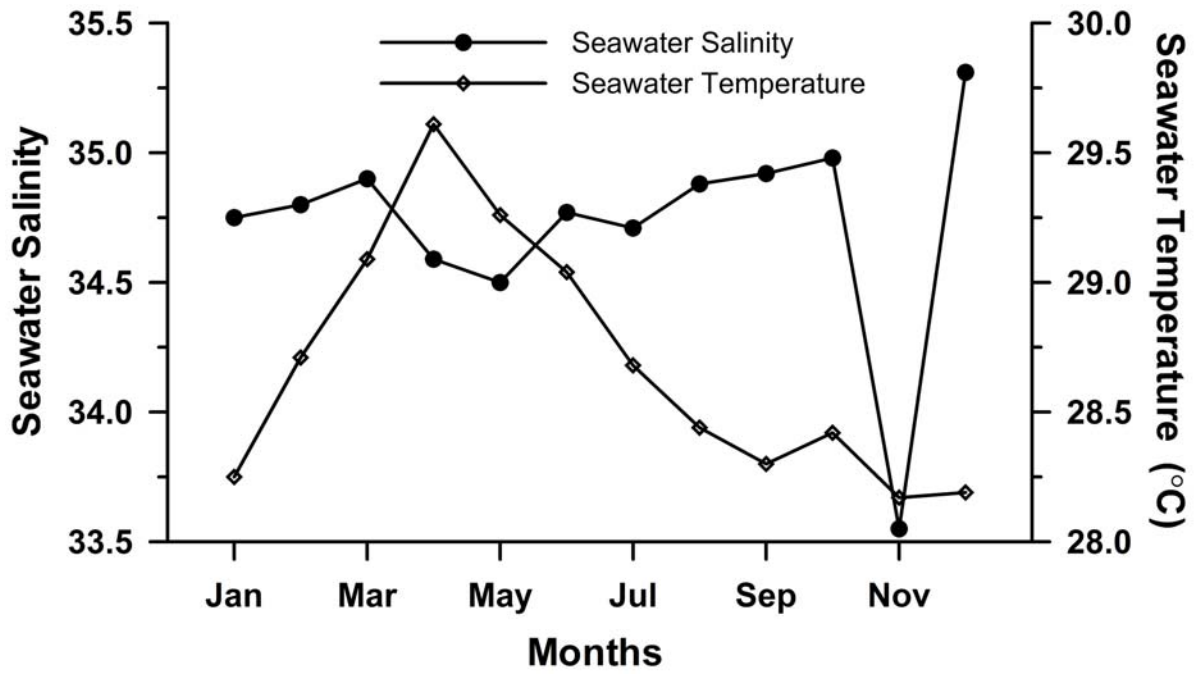


Figure 4

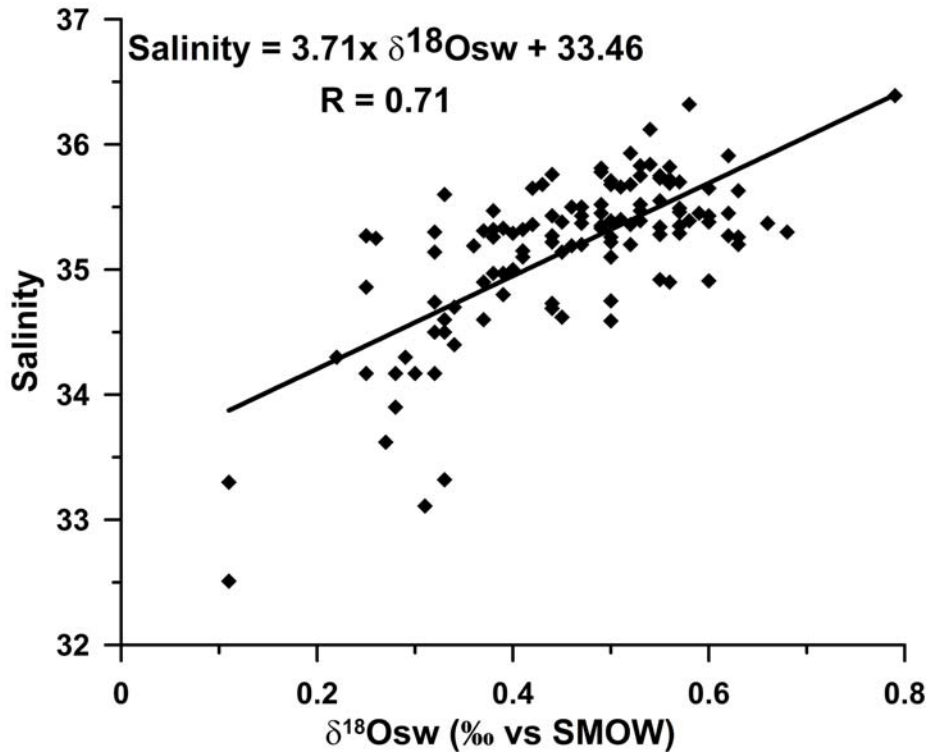


Figure 5

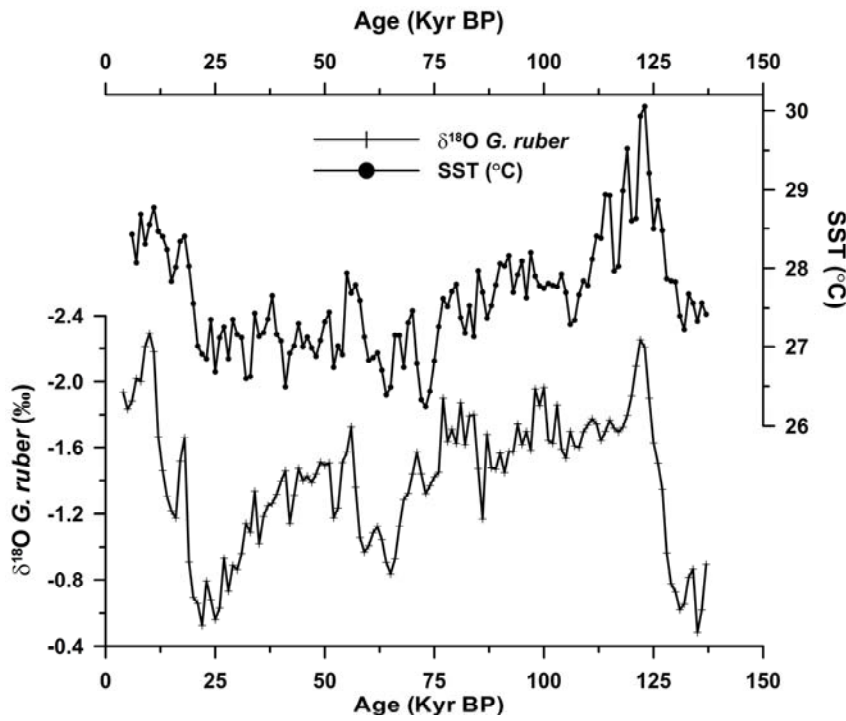


Figure 6

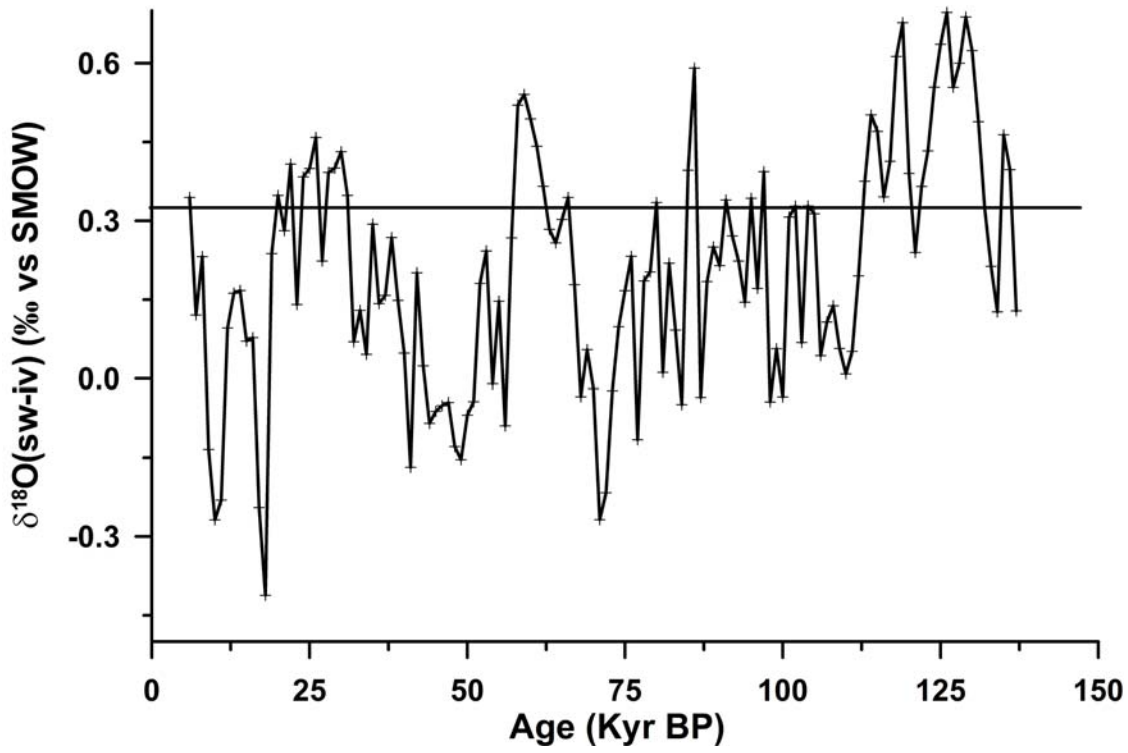


Figure 7

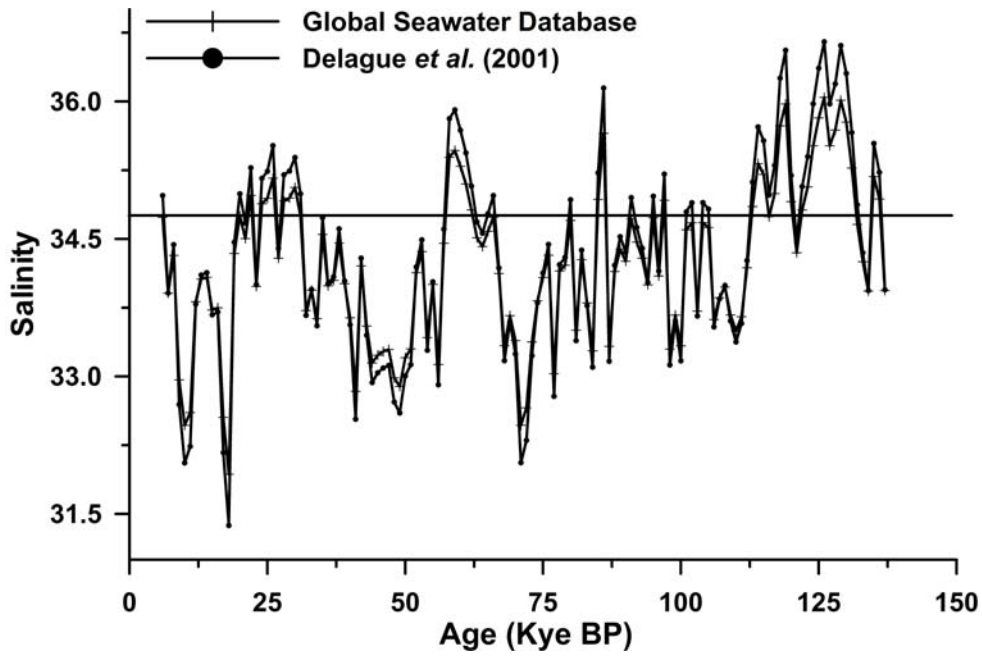


Figure 8

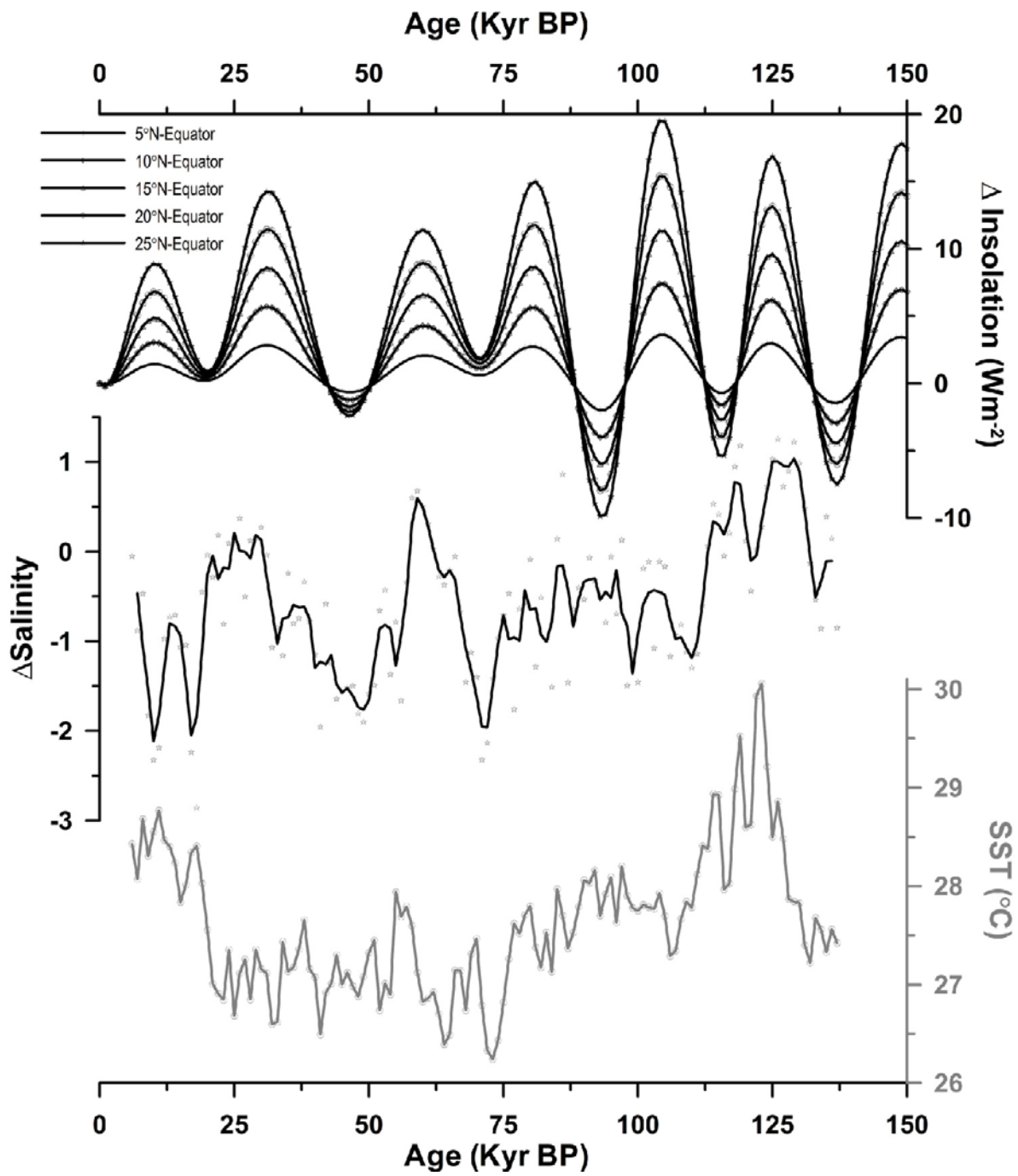


Figure 9

